Performance Analysis of FSO Communications with Diversity Methods: Add More Relays or More Apertures?

Chadi Abou-Rjeily, *Senior Member IEEE*

***Abstract*—This paper targets the performance analysis of Multiple-Input-Multiple-Output (MIMO) point-to-point, single-aperture relay-assisted and MIMO relay-assisted Free-Space Optical (FSO) communications. The objective of the paper is to compare the different FSO diversity methods via an outage probability analysis over gamma-gamma turbulence channels in the case of independent fading among the different apertures of the communicating nodes. Through a well-tailored calculation method, we approximate the gamma-gamma distribution and the gamma-gamma sum-distribution by appropriate gamma distributions. This method resulted in simple closed-form outage probability expressions that are accurate for average-to-large values of the signal-to-noise ratio (SNR) and in asymptotic expressions that are useful for evaluating the diversity gains and coding gains. In particular, we derived the diversity gains of MIMO repetition coding (RC), MIMO transmit laser selection (TLS), MIMO all-active relaying (AR) and MIMO selective-relaying (SR). We prove that MIMO-RC and MIMO-TLS, on one hand, and MIMO-AR and MIMO-SR, on the second hand, achieve the same diversity gain and we evaluate the coding gain of TLS with respect to RC and of SR with respect to AR. By comparing the MIMO and cooperative methods with point receivers, we reach the central result that it is always better, from a diversity gain point of view, to add more apertures to the source and destination rather than adding more relays in their vicinity despite the fact that the fading variance along FSO links decreases with the distance. For receivers that implement aperture averaging, we derive conditions under which MIMO techniques are unconditionally better than cooperative techniques with any network topology.**

***Index Terms*—Free-space optics, FSO, MIMO, cooperation, relaying, relay-assisted, fading, diversity, gamma-gamma.**

I. Introduction

Multiple-Input-Multiple-Output (MIMO) techniques and relay-assisted communications constitute two popular fading mitigation techniques that were studied extensively in the context of Free-Space Optical (FSO) systems. MIMO systems are localized diversity methods where several transmit apertures (lasers) and receive apertures (photodiodes) are placed at the transmitter and receiver sides, respectively. MIMO FSO systems were associated with either repetition coding (RC) [1], [2] or transmit laser selection (TLS) [3], [4]. For RC, the same information symbol is transmitted from all apertures and this solution can be implemented in the absence of channel state information (CSI) and feedback. In contrast to RC, the TLS solution corresponds to activating the laser ensuring the maximum irradiance at the receiver and this solution requires a feedback link as well as acquiring the CSI. On the other hand, relay-assisted methods constitute distributed spatial diversity solutions where neighboring nodes (or relays denoted by R) assist the communications between a source node (S) and a destination node (D). Of particular interest are the parallel-relaying decode-and-forward solutions [5]–[17]. In a way analogous to the MIMO-RC and MIMO-TLS methods, all-active [5]–[14] and selective relaying [15]–[17] solutions were proposed and analyzed. For all-active relaying, all neighboring relays forward the decoded message to the destination, while for selective-relaying, the strongest relay is selected. While selective-relaying is superior to all-active relaying, the implementation of the former requires acquiring the CSI of all intermediate channels as well as adding feedback links between the communicating nodes.

Despite the huge literature on MIMO and relay-assisted FSO systems, these techniques were neither compared nor combined before. In this paper, we analyze the performance of MIMO systems as well as all-active and selective relaying in the case where the intermediate links between the different nodes are equipped with multiple apertures. The performance is evaluated via an outage probability analysis over gamma-gamma atmospheric turbulence FSO links where the parallel-relaying scheme is considered. The system model of parallel-relaying is depicted in Fig. 1 where the transmission between a pair of nodes in the network is performed by using a dedicated pair of transceivers each equipped with multiple apertures. Of direct relevance to this paper is the work presented in [9]–[11] in the case of all-active relaying. In [9], an outage analysis was performed with one relay. The diversity gain with any number of relays was derived in [10] through an average error probability analysis. Moreover, the diversity gains and diversity-multiplexing tradeoffs of all-active relaying with one relay were evaluated in [11]. While [9]–[11] all consider gamma-gamma channels, the main difference with our work is as follows. First, Single-Input-Single-Output (SISO) links were considered in [9]–[11] while our work considers the more general case of MIMO links. The second difference resides in the detection/combining scheme implemented at the destination in the case of all-active relaying. Unlike [9]–[11] where the signals falling on the different transceivers placed at D are detected separately, these signals are added up prior to detection in this work. The adopted diversity combining scheme is superior to the switching scheme considered in [9]–[11] where D consents the decision made by any of its

The author is with the Department of Electrical and Computer Engineering of the Lebanese American University (LAU), Byblos, Lebanon. (e-mail: chadi.abourjeily@lau.edu.lb).

receivers that are not in outage. For the scheme considered in this work, even if the links R_i-D and R_j-D are in outage, yet the superposition of the signals transmitted from R_i and R_j to D can still not be in outage resulting in a superior performance.

The diversity combining scheme adopted in this paper is the same as the one proposed initially in [12] and that was further analyzed in [13]–[15]. In [12]–[15], D is equipped with a single aperture having a wide field of view where the signals transmitted from S and the relays get superimposed at D. The performance analysis with this combining scheme is more challenging since it involves the evaluation of the probability density function (pdf) or cumulative distribution function (cdf) of the weighted sum of a certain number of random variables corresponding to the square of the path gains. The analysis in [12]–[14] holds for lognormal fading channels where, using conventional tools, the above sum of a number of lognormal random variables can be further approximated by another lognormal random variable which substantially simplifies the analysis. On the other hand, [15] considered a gamma-gamma fading model; however, in the case of all-active relaying the gamma-gamma sum-cdf was evaluated numerically thus limiting the interest of the adopted approach. Moreover, an expression for the achievable diversity gain with the combining scheme is still missing.

The main contributions of this paper are two-fold. First, we evaluate the outage performance of MIMO relay-assisted FSO systems with all-active (deploying diversity combining at D) and selective relaying over gamma-gamma fading channels where these schemes were associated with RC and TLS, respectively. Based on this analysis, we derive the diversity gains achieved by both relaying strategies and we prove that they are the same while quantifying the superiority of selective relaying in a closed-form expression of the coding gain that we derive. To the author's best knowledge, despite the rich literature on all-active relaying [5]–[14] and selective-relaying [15]–[17], it was not demonstrated before that these strategies are capable of achieving the same diversity gain nor was the coding gain previously derived. The second contribution resides in proving that MIMO systems are strictly superior to relay-assisted systems under the constraint of the same total number of apertures with point receivers and in the case where the relays are added for the mere objective of assisting S in its communication with D as in [12]–[15]. In other words, if the transmit (resp. receive) apertures were removed from the relays and placed at S (resp. D), then the diversity gain will be enhanced. It is worth noting that this diversity gain is associated with a reduced system complexity where adding apertures to the transmitter or to the receiver is much more cost-effective than deploying relays thus proving the inadequacy of this last approach to FSO systems. On the other hand, if the relays are independent entities that have their own information to exchange with S and D as in [5]–[11], [16], [17], then taking advantage of the presence of these relays (that can not be removed since they are not deployed solely for assisting S) can not but improve the reliability of the communications between S and D. Other contributions include deriving the diversity gains of MIMO systems with RC and TLS as well as the coding gain of TLS compared to RC which constitute novel findings as well. We also study the impact of aperture averaging on the derived results.

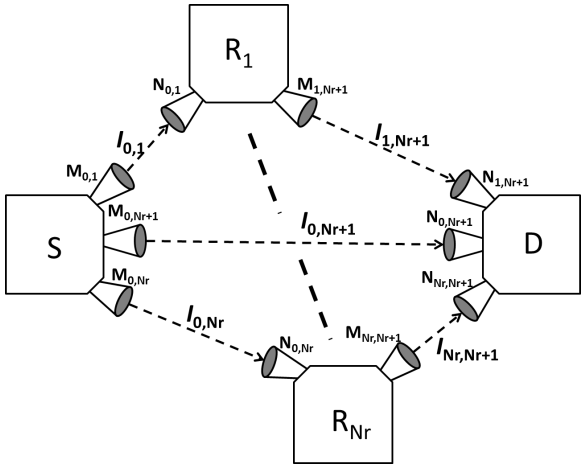

Fig. 1. A cooperative FSO network with N_r relays.

The closed-form outage probabilities, diversity gains and coding gains derived in this paper are based on the calculation methodology proposed in [18]. In this context, the gamma-gamma pdf is approximated by a gamma pdf near the origin. This calculation method is suitable for the analysis of MIMO (resp. all-active relaying) systems that involves the summation of identically (resp. non-identically) distributed gamma-gamma random variables and that, hence, can be approximated by a conveniently-scaled gamma distribution. The adopted method is also of crucial importance since it results in closed-form expressions that are accurate over a wide range of the signal-to-noise ratio (SNR); these expressions do not entail series with infinite number of terms and only conventional mathematical functions appear in the final results.

II. System Model

Consider the cooperative FSO network with N_r relays shown in Fig. 1. For communicating along the link R_i-R_j, $M_{i,j}$ transmit apertures are placed at R_i while $N_{i,j}$ receive apertures are placed at R_j. For notational simplicity, S and D will be denoted by R_0 and R_{N_r+1}, respectively. The FSO system under consideration employs Binary Pulse Position Modulation (BPPM) with Intensity-Modulation and Direct-Detection (IM/DD). This paper targets mainly the case of point receivers that do not deploy aperture averaging. The case of aperture averaging will be considered separately in section VI.

The received electrical signal at the j-th node resulting from the optical signal transmitted by the i-th node can be written as [12]:

$$\mathfrak{r}_{i,j} = \begin{bmatrix} \mathfrak{r}^{\mathrm{s}}_{i,j} \\ \mathfrak{r}^{\mathrm{n}}_{i,j} \end{bmatrix} = \begin{bmatrix} RT_b(G_{i,j} r_{i,j} \mathcal{I}_{i,j} P_t + P_b) + \mathfrak{n}^{\mathrm{s}}_j \\ RT_b P_b + \mathfrak{n}^{\mathrm{n}}_j \end{bmatrix} \quad (1)$$

where $\mathfrak{r}^{\mathrm{s}}_{i,j}$ and $\mathfrak{r}^{\mathrm{n}}_{i,j}$ are the received electrical signals that correspond to the signal and non-signal slots of the BPPM symbol, respectively. R is the photodetector's responsivity and T_b stands for the bit duration. P_b stands for the power of background radiation while P_t stands for the total transmitted optical signal power. $r_{i,j}$ is a power normalization factor that

stands to the fraction of the total power allocated to the link R_i-R_j. $\mathfrak{n}_j^s$ and $\mathfrak{n}_j^n$ stand for the additive noise terms at R_j in the signal and non-signal slots, respectively. As in [12], we assume background noise limited receivers implying that each of the above noise terms can be modeled as a signal-independent white Gaussian noise with zero mean and variance $N_0/2$ in the case where R_j is equipped with one receive aperture.

In this work, we adopt the gamma-gamma fading model where the pdf of the irradiance ($I \geq 0$) is given by:

$$f_{\gamma\gamma}(I) = \frac{2(\alpha\beta)^{(\alpha+\beta)/2}}{\Gamma(\alpha)\Gamma(\beta)} I^{(\alpha+\beta)/2-1} K_{\alpha-\beta}\left(2\sqrt{\alpha\beta I}\right) \quad (2)$$

where $\Gamma(.)$ is the Gamma function and $K_c(.)$ is the modified Bessel function of the second kind of order c. The parameters α and β with point receivers are given by:

$$\alpha(d) = \left[\exp\left(0.49\sigma_R^2(d)/(1+1.11\sigma_R^{12/5}(d))^{7/6}\right) - 1\right]^{-1} \quad (3)$$

$$\beta(d) = \left[\exp\left(0.51\sigma_R^2(d)/(1+0.69\sigma_R^{12/5}(d))^{5/6}\right) - 1\right]^{-1} \quad (4)$$

where $\sigma_R^2(d) = 1.23C_n^2k^{7/6}d^{11/6}$ is the Rytov variance, d is the link distance, k is the wave number and C_n^2 denotes the refractive index structure parameter. From(3)-(4), the parameters of the link between nodes i and j can be written as:

$$\alpha_{i,j} \triangleq \alpha(d_{i,j}) \quad ; \quad \beta_{i,j} \triangleq \beta(d_{i,j}) \quad (5)$$

where $d_{i,j}$ stands for the distance between R_i and R_j.

MIMO all-active relaying will be associated with RC and this system can be implemented in the absence of feedback and CSI. On the other hand, MIMO selective-relaying will be associated with the TLS scheme where this system achieves higher performance levels at the expense of entailing feedback communications and necessitating the knowledge of the CSI. The term $\mathcal{I}_{i,j}$ in (1) depends on the implemented MIMO scheme and can be written as [1]–[4]:

$$\mathcal{I}_{i,j} = \begin{cases} \frac{1}{M_{i,j}} \sum_{m=1}^{M_{i,j}} \sum_{n=1}^{N_{i,j}} I_{i,j}^{(m,n)}, & \text{MIMO-RC;} \\ \max_{m=1,\ldots,M_{i,j}} \sum_{n=1}^{N_{i,j}} I_{i,j}^{(m,n)}, & \text{MIMO-TLS.} \end{cases} \quad (6)$$

where $I_{i,j}^{(m,n)}$ stands for the irradiance between the m-th transmit aperture of R_i and the n-th receive aperture of R_j.

The normalization by $M_{i,j}$ in (6) with RC, where all laser sources are transmitting the same symbol, ensures the same transmission level as in the case of SISO links. Note that with TLS, this normalization is not needed since only one laser source is emitting. In the case where $N_{i,j} > 1$, since the optical signals falling on the receive apertures are added up, then the variance of the noise terms $\mathfrak{n}_j^s$ and $\mathfrak{n}_j^n$ in (1) would be equal to $N_{i,j}N_0/2$ where it is assumed that the noise terms at the different receive apertures are independent.

Finally, $G_{i,j}$ in (1) is a gain factor associated with the link R_i-R_j that might be shorter than the direct link S-D. In this context, $G_{0,N_r+1} = 1$ and from [12]:

$$G_{i,j} = \left(\frac{d_{0,N_r+1}}{d_{i,j}}\right)^2 e^{-\sigma(d_{i,j}-d_{0,N_r+1})} \quad (7)$$

where σ is the attenuation coefficient.

In what follows, the refractive index structure constant and the attenuation constant are set to $C_n^2 = 1.7\times10^{-14}$ m$^{-2/3}$ and $\sigma = 0.43$ dB/km, respectively. The operating wavelength is set to 1550 nm.

After removing the constant bias RT_bP_b from both BPPM slots in (1), the SNR of the link R_i-R_j can be written as [12]:

$$\gamma_{i,j} = \frac{R^2T_b^2G_{i,j}^2r_{i,j}^2\mathcal{I}_{i,j}^2P_t^2}{N_{i,j}N_0} \quad (8)$$

The outage probability of the link R_i-R_j can be written as:

$$p_{i,j} \triangleq \Pr\left(\gamma_{i,j} < \gamma_{th}\right) = \Pr\left(\mathcal{I}_{i,j} < \left[\frac{G_{i,j}r_{i,j}P_M}{\sqrt{N_{i,j}}}\right]^{-1}\right) \quad (9)$$

where $P_M \triangleq \frac{RT_bP_t}{\sqrt{N_0\gamma_{th}}}$ denotes the power margin and γ_{th} is the SNR threshold above which no outage occurs and the signal can be decoded with an arbitrarily small probability of error.

The diversity gain $d_{i,j}$ is defined as the negative slope of the curve $p_{i,j}(P_M)$ on a log-log plot for large values of P_M [19]:

$$d_{i,j} = -\lim_{P_M\to\infty} \frac{\log(p_{i,j})}{\log(P_M)} \quad (10)$$

in other words, the outage probability along the link R_i-R_j will vary asymptotically as $P_M^{-d_{i,j}}$ for large values of P_M.

III. Performance Analysis of SISO, MIMO and Multi-Source Transmissions

A. Performance Analysis of SISO Links

At a first time, we examine the FSO link between nodes R_i and R_j. We consider the case where R_i is equipped with $M_{i,j} = 1$ laser source and R_j is equipped with $N_{i,j} = 1$ photodetector. In this case, (9) can be written as:

$$p_{i,j} = \Pr\left(I_{i,j} < [G_{i,j}r_{i,j}P_M]^{-1}\right) \quad (11)$$

where $\mathcal{I}_{i,j} \triangleq I_{i,j}^{(1,1)}$ was written as $I_{i,j}$ for simplicity.

Given that $I_{i,j}$ is gamma-gamma distributed, then (11) can be evaluated in terms of the Meijer G-function using the cdf of the gamma-gamma distribution [11]. However, the Meijer G-function is difficult to tackle mathematically and, consequently, the obtained results will fail in offering clear and intuitive insights on the performance over the FSO link. Moreover, this approach can not be further extended to the scenarios of MIMO and multi-source transmissions, as will be explained later.

Based on the above, we next resort to approximate the gamma-gamma pdf in (2). By using the power series expansion of the modified Bessel function near the origin, (2) can be approximated by [20]:

$$f_{\gamma\gamma}(I) \approx a_0I^{\beta-1} + a_1I^{\beta} \quad (12)$$

where only the first two terms in the power series expansion were considered and where:

$$a_0 = \frac{\Gamma(\alpha-\beta)}{\Gamma(\alpha)\Gamma(\beta)}(\alpha\beta)^{\beta} \quad ; \quad a_1 = \frac{\Gamma(\alpha-\beta)}{\Gamma(\alpha)\Gamma(\beta)}\frac{(\alpha\beta)^{\beta+1}}{(1-\alpha+\beta)} \quad (13)$$

The key step in our subsequent calculations resides in writing (12) as $a_0I^{\beta-1}\left(1+\frac{a_1}{a_0}I\right)$ which can be further approximated by $a_0I^{\beta-1}e^{\frac{a_1}{a_0}I}$ where the approximation methodology

proposed in [18] was adopted. This methodology resides in approximating the exponential function near the origin by the first two terms of the Taylor series expansion so that the obtained function can be related to the gamma pdf. Replacing a_0 and a_1 by their values from (13), the pdf of the irradiance along R_i-R_j around the origin can be advantageously approximated by:

$$f_{\gamma\gamma}(I) \approx C_{i,j} f_{\gamma}(I, \beta_{i,j}, A_{i,j}) \tag{14}$$

where $f_{\gamma}(I,k,\theta) = \frac{1}{\Gamma(k)\theta^k} I^{k-1} e^{-x/\theta}$ stands for the gamma pdf with shape parameter k and scale parameter θ. In (14), $C_{i,j}$ and $A_{i,j}$ are two constants related to the parameters $\alpha_{i,j}$ and $\beta_{i,j}$ of the link R_i-R_j by:

$$C_{i,j} = \frac{(\alpha_{i,j} - \beta_{i,j} - 1)^{\beta_{i,j}} \Gamma(\alpha_{i,j} - \beta_{i,j})}{\Gamma(\alpha_{i,j})} \tag{15}$$

$$A_{i,j} = \frac{\alpha_{i,j} - \beta_{i,j} - 1}{\alpha_{i,j}\beta_{i,j}} \tag{16}$$

Note that the function to the right hand-side of (14) is not a pdf since the area under this function is equal to $C_{i,j} \neq 1$. However, this function better approximates the exact pdf $f_{\gamma\gamma}(I)$ near the origin resulting in accurate approximations of the outage probability for average-to-large values of the SNR.

From (14), the outage probability in (11) can be evaluated using the cdf of the gamma distribution as follows:

$$p_{i,j} \approx \frac{C_{i,j}}{\Gamma(\beta_{i,j})} \gamma\left(\beta_{i,j}, [A_{i,j} G_{i,j} r_{i,j} P_M]^{-1}\right) \tag{17}$$

where $\gamma(s,x) = \int_0^x t^{s-1} e^{-t} \mathrm{d}t$ stands for the lower incomplete gamma function.

Besides its usefulness in evaluating the performance of MIMO and cooperative systems, (17) is a new result that is beneficial for writing the outage probability of a point-to-point SISO FSO link with parameters α and β in closed form as:

$$P_{out} \approx \frac{(\alpha - \beta - 1)^{\beta} \Gamma(\alpha - \beta)}{\Gamma(\alpha)\Gamma(\beta)} \gamma\left(\beta, \frac{\alpha\beta}{\alpha - \beta - 1} P_M^{-1}\right) \tag{18}$$

where, for the point-to-point link, $G_{i,j} = 1$ and $r_{i,j} = 1$.

Using the relation $\gamma(s,x) \approx \frac{x^s}{s}$ for small values of x, (17) can be further approximated by the following expression for large values of P_M:

$$p_{i,j} \approx \frac{\Gamma(\alpha_{i,j} - \beta_{i,j})}{\Gamma(\alpha_{i,j})\Gamma(\beta_{i,j})} \frac{(\alpha_{i,j}\beta_{i,j})^{\beta_{i,j}}}{\beta_{i,j}} (G_{i,j} r_{i,j} P_M)^{-\beta_{i,j}} \tag{19}$$

implying that the outage probability of a point-to-point SISO FSO link in (18) tends asymptotically to:

$$P_{out} \approx \frac{\Gamma(\alpha - \beta)(\alpha\beta)^{\beta}}{\Gamma(\alpha)\Gamma(\beta + 1)} P_M^{-\beta} \tag{20}$$

showing that the diversity gain is equal to β. While expressions similar to (20) were previously reported in the literature [17], to the author's best knowledge, approximations in the form of (18) are novel.

In Fig. 2, we compare the exact outage probability with the approximate and asymptotic expressions in (18) and (20) for various link distances. Results show that the closed-form and simple expression in (18) is extremely close to the exact outage probability over the entire range of P_M for the link

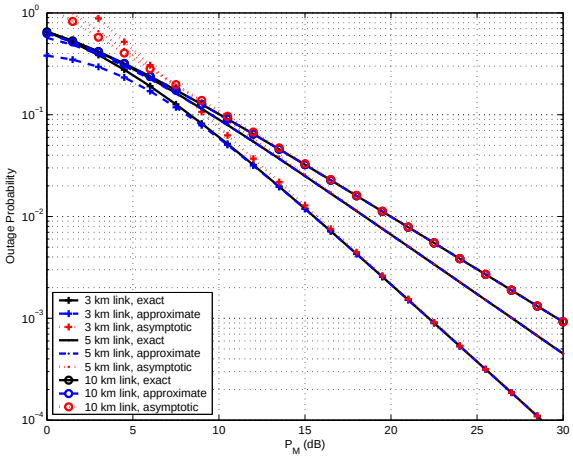

Fig. 2. Outage probability over SISO FSO links.

distances of 5 km and 10 km. For the shorter link distance of 3 km that suffers from lower levels of fading, (18) accurately predicts the outage probability for values of P_M exceeding 7.5 dB. In this scenario, (20) is close to the exact expression for values of P_M exceeding 15 dB while it is very far from the exact expression for smaller values of P_M. Moreover, this asymptotic expression suffers from the fact that it exceeds 1 for extremely small values of P_M. Fig. 2 shows the interest of the adopted calculation approach where the new expression derived in (18) accurately predicts the performance of SISO FSO links over a wide range of values of P_M.

B. Performance Analysis of MIMO Links

For MIMO links, $\{I_{i,j}^{(m,n)}\}_{m,n}$ are identically distributed according to a gamma-gamma distribution with parameters $\alpha_{i,j}$ and $\beta_{i,j}$. Our subsequent calculations are based on the assumption that these irradiances are independent as well. This assumption holds for the scenario where the elements of the transmit and receive arrays are sufficiently spaced resulting in independent channel fades.

1) Repetition coding (RC), no feedback: From (6) and (9), the outage probability of the link R_i-R_j can be written as:

$$p_{i,j} = \Pr\left(\sum_{m=1}^{M_{i,j}} \sum_{n=1}^{N_{i,j}} I_{i,j}^{(m,n)} < \left[\frac{G_{i,j} r_{i,j} P_M}{M_{i,j}\sqrt{N_{i,j}}}\right]^{-1}\right) \tag{21}$$

From (14), given that each one of the terms $I_{i,j}^{(m,n)}$ can be approximated by a gamma distribution, and following from the fact that the sum of independent gamma random variables with the same scale parameter is a gamma random variable having the same scale parameter and a shape parameter equal to the sum of the shape parameters, the pdf of $\sum_{m,n} I_{i,j}^{(m,n)}$ can be approximated as follows:

$$f_{\sum_{m,n} I_{i,j}^{(m,n)}}(I) \approx C_{i,j}^{M_{i,j}N_{i,j}} f_{\gamma}(I, M_{i,j}N_{i,j}\beta_{i,j}, A_{i,j}) \tag{22}$$

which shows the interest of the adopted approach in approximating a gamma-gamma pdf by a gamma pdf. (22) implies

that (21) can be approximated by:

$$p_{i,j} \approx \frac{C_{i,j}^{M_{i,j}N_{i,j}}}{\Gamma(M_{i,j}N_{i,j}\beta_{i,j})}\gamma\left(M_{i,j}N_{i,j}\beta_{i,j}, \left[\frac{A_{i,j}G_{i,j}r_{i,j}P_M}{M_{i,j}\sqrt{N_{i,j}}}\right]^{-1}\right) \quad (23)$$

which tends asymptotically to:

$$p_{i,j} \approx \frac{C_{i,j}^{M_{i,j}N_{i,j}}}{\Gamma(M_{i,j}N_{i,j}\beta_{i,j}+1)}\left[\frac{A_{i,j}G_{i,j}r_{i,j}P_M}{M_{i,j}\sqrt{N_{i,j}}}\right]^{-M_{i,j}N_{i,j}\beta_{i,j}} \quad (24)$$

Results in the form of (23) and (24) are novel and of particular interest for expressing the outage probability over gamma-gamma MIMO links in closed-form. From (23), the outage probability of a $M \times N$ MIMO FSO link deploying RC over a gamma-gamma fading channel with parameters α and β can be written as:

$$P_{out} \approx \frac{1}{\Gamma(MN\beta)}\left[\frac{(\alpha-\beta-1)^{\beta}\Gamma(\alpha-\beta)}{\Gamma(\alpha)}\right]^{MN} \gamma\left(MN\beta, \frac{\alpha\beta}{\alpha-\beta-1}\left(\frac{P_M}{M\sqrt{N}}\right)^{-1}\right) \quad (25)$$

which, from (24), tends asymptotically to:

$$P_{out} \approx \frac{1}{\Gamma(MN\beta+1)}\left[\frac{\Gamma(\alpha-\beta)(\alpha\beta)^{\beta}}{\Gamma(\alpha)}\right]^{MN}\left(\frac{P_M}{M\sqrt{N}}\right)^{-MN\beta} \quad (26)$$

where $C_{i,j}$ and $A_{i,j}$ were replaced by their values from (15) and (16), respectively, and where we set $G_{i,j}=1$ and $r_{i,j}=1$. Replacing $M=N=1$ in (25) and (26) results in (18) and (20), respectively.

2) Transmit laser selection, with feedback: From (6) and (9), the outage probability of the link R_i-R_j can be written as:

$$\begin{aligned} p_{i,j} &= \Pr\left(\max_{m=1,\ldots,M_{i,j}}\sum_{n=1}^{N_{i,j}} I_{i,j}^{(m,n)} < \left[\frac{G_{i,j}r_{i,j}P_M}{\sqrt{N_{i,j}}}\right]^{-1}\right) \\ &= \prod_{m=1}^{M_{i,j}}\Pr\left(\sum_{n=1}^{N_{i,j}} I_{i,j}^{(m,n)} < \left[\frac{G_{i,j}r_{i,j}P_M}{\sqrt{N_{i,j}}}\right]^{-1}\right) \\ &= \left[\Pr\left(\sum_{n=1}^{N_{i,j}} I_{i,j}^{(m,n)} < \left[\frac{G_{i,j}r_{i,j}P_M}{\sqrt{N_{i,j}}}\right]^{-1}\right)\right]^{M_{i,j}} \end{aligned} \quad (27)$$

where the last two equations follow since $I_{i,j}^{(m,n)}$ are independent and identically distributed for $m=1,\ldots,M_{i,j}$ and $n=1,\ldots,N_{i,j}$.

In a way similar to (22), and since $\sum_{n=1}^{N_{i,j}} I_{i,j}^{(m,n)}$ can be approximated by the sum of $N_{i,j}$ independent gamma random variables with the same scale parameter $A_{i,j}$, then the pdf of this random variable can be approximated by:

$$f_{\sum_n I_{i,j}^{(m,n)}}(I) \approx C_{i,j}^{N_{i,j}} f_{\gamma}(I, N_{i,j}\beta_{i,j}, A_{i,j}) \quad (28)$$

implying that (27) can be written as:

$$p_{i,j} \approx \left[\frac{C_{i,j}^{N_{i,j}}}{\Gamma(N_{i,j}\beta_{i,j})}\gamma\left(N_{i,j}\beta_{i,j}, \left[\frac{A_{i,j}G_{i,j}r_{i,j}P_M}{\sqrt{N_{i,j}}}\right]^{-1}\right)\right]^{M_{i,j}} \quad (29)$$

which tends asymptotically to:

$$p_{i,j} \approx \frac{C_{i,j}^{M_{i,j}N_{i,j}}}{[\Gamma(N_{i,j}\beta_{i,j}+1)]^{M_{i,j}}}\left[\frac{A_{i,j}G_{i,j}r_{i,j}P_M}{\sqrt{N_{i,j}}}\right]^{-M_{i,j}N_{i,j}\beta_{i,j}} \quad (30)$$

Equations (29) and (30) constitute additional contributions of this work where the outage probability of a $M \times N$ MIMO FSO link deploying the TLS scheme over a gamma-gamma fading channel with parameters α and β can be expressed as:

$$P_{out} \approx \frac{1}{[\Gamma(N\beta)]^M}\left[\frac{(\alpha-\beta-1)^{\beta}\Gamma(\alpha-\beta)}{\Gamma(\alpha)}\right]^{MN} \left[\gamma\left(N\beta, \frac{\alpha\beta}{\alpha-\beta-1}\left(\frac{P_M}{\sqrt{N}}\right)^{-1}\right)\right]^{M} \quad (31)$$

and where the corresponding asymptotic approximation is:

$$P_{out} \approx \frac{1}{[\Gamma(N\beta+1)]^M}\left[\frac{\Gamma(\alpha-\beta)(\alpha\beta)^{\beta}}{\Gamma(\alpha)}\right]^{MN}\left(\frac{P_M}{\sqrt{N}}\right)^{-MN\beta} \quad (32)$$

where $C_{i,j}$ and $A_{i,j}$ were replaced by their values from (15) and (16), respectively, and where we set $G_{i,j}=1$ and $r_{i,j}=1$. Replacing $M=N=1$ in (31) and (32) results in (18) and (20), respectively.

3) Diversity gain and coding gain: Equations (26) and (32) show that the diversity gain of an $M \times N$ MIMO FSO link over a gamma-gamma channel with parameters α and β is equal to $MN\beta$ whether RC or TLS is deployed. In other words, the presence of feedback does not enhance the diversity gain as expected.

Writing the outage probabilities in (26) and (32) in the form $(g_c P_M)^{-\nu}$ where ν is the diversity gain (equal to $MN\beta$) and g_c is the coding gain, we can deduce that the advantage of TLS over RC resides in a coding gain of:

$$10\log_{10}\left(M\left[\frac{\Gamma(N\beta+1)}{[\Gamma(MN\beta+1)]^{\frac{1}{M}}}\right]^{\frac{1}{N\beta}}\right) \quad \text{(dB)} \quad (33)$$

A numerical analysis of (33) shows that the coding gain is an increasing function of M and the link distance (decreasing function of β) while it is a decreasing function of N.

In Fig. 3, we compare the exact outage probability with the derived approximate and asymptotic expressions given in (25)-(26) and (31)-(32) for RC and TLS, respectively. We consider a link distance of 3 km resulting in $\beta = 1.53$. Results show the accuracy of the approximate expressions for average-to-large values of P_M and of the asymptotic expressions for large values of P_M. While the asymptotic expressions exhibit a slow convergence towards the exact outage probability especially for 3×3 systems, the approximate expressions are characterized by a faster convergence where, for example, they can correctly predict the performance of 3×3 systems for values of P_M exceeding 8 dB. As predicted by our calculations, the diversity gain is equal to 6.12 and 13.77 with 4×1 and 3×3 systems, respectively, whether in the absence or presence of feedback. Moreover, as predicted by (33), TLS results in coding gains of 2.06 dB and 0.9 dB compared to RC with 4×1 and 3×3 systems, respectively. Results shown in Fig. 4 for a link distance of 5 km show that the accuracy of the

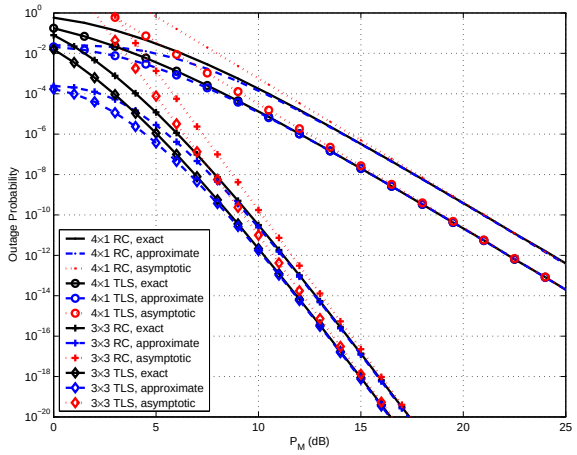

Fig. 3. Outage probability over 3 km MIMO FSO links.

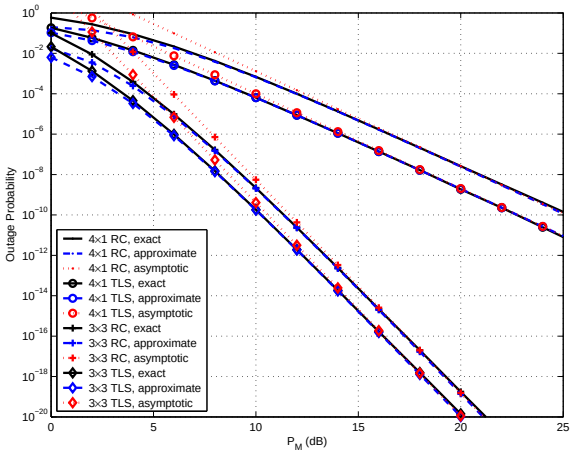

Fig. 4. Outage probability over 5 km MIMO FSO links.

approximate expressions in (25) and (31) is further enhanced with increased link distances. The coding gains increase to 2.37 dB and 1.07 dB for 4×1 and 3×3 systems, respectively.

C. Performance Analysis of Multi-Source Transmissions

The utility of (14) resides in the fact that it lends itself to the analysis of multi-source (MS) transmissions as well. This analysis of the MS transmissions constitutes an intermediate step for the outage analysis of cooperative networks with all-active relaying. Consider the case where the nodes $\{\mathrm{R}_i\}_{i\in\mathcal{S}}$ are transmitting the same PPM symbol simultaneously to the node R_j. In a way similar to (8), this multi-source transmission results in the following expression for the SNR at R_j:

$$\gamma_{\mathcal{S},j}=\frac{R^2T_b^2\mathcal{I}_{\mathcal{S},j}^2P_t^2}{N_0\sum_{i\in\mathcal{S}}N_{i,j}} \tag{34}$$

where the random variable $\mathcal{I}_{\mathcal{S},j}$ takes the following form:

$$\mathcal{I}_{\mathcal{S},j}=\sum_{i\in\mathcal{S}}\frac{G_{i,j}r_{i,j}}{M_{i,j}}\sum_{m=1}^{M_{i,j}}\sum_{n=1}^{N_{i,j}}I_{i,j}^{(m,n)} \tag{35}$$

where since (14) follows as a special case from (22) by setting $M_{i,j}=N_{i,j}=1$, we considered the general case of MIMO nodes in (35).

The distribution of $\sum_{m,n}I_{i,j}^{(m,n)}$ can be approximated as in (22) and the random variable $\mathcal{I}_{\mathcal{S},j}$ can be approximated by the weighted sum of $|\mathcal{S}|$ independent and non-identically distributed gamma random variables. We adopt the approach proposed in [18] for approximating the pdf of $\mathcal{I}_{\mathcal{S},j}$ by a conveniently-scaled gamma pdf. Given that the random variables appearing in the summation to the right-hand side of (35) are independent, then the moment generating function (mgf) $\mathcal{M}_{\mathcal{I}_{\mathcal{S},j}}(s)=\mathrm{E}\left[e^{-s\mathcal{I}_{\mathcal{S},j}}\right]$ can be written as:

$$\mathcal{M}_{\mathcal{I}_{\mathcal{S},j}}(s)=\prod_{i\in\mathcal{S}}\mathcal{M}_{\sum_{m,n}I_{i,j}^{(m,n)}}\left(\frac{G_{i,j}r_{i,j}}{M_{i,j}}s\right) \tag{36}$$

$$=\prod_{i\in\mathcal{S}}C_{i,j}^{M_{i,j}N_{i,j}}\left(1+\frac{G_{i,j}r_{i,j}}{M_{i,j}}A_{i,j}s\right)^{-M_{i,j}N_{i,j}\beta_{i,j}} \tag{37}$$

where (37) follows from the mgf of the gamma pdf in (22) and where $C_{i,j}$ and $A_{i,j}$ are given in (15) and (16), respectively.

Expanding (37) for large values of s:

$$\mathcal{M}_{\mathcal{I}_{\mathcal{S},j}}(s)=\left[\prod_{i\in\mathcal{S}}C_{i,j}^{M_{i,j}N_{i,j}}\right]\prod_{i\in\mathcal{S}}\left[\left(\frac{M_{i,j}}{G_{i,j}r_{i,j}A_{i,j}s}\right)^{M_{i,j}N_{i,j}\beta_{i,j}}-M_{i,j}N_{i,j}\beta_{i,j}\left(\frac{M_{i,j}}{G_{i,j}r_{i,j}A_{i,j}s}\right)^{M_{i,j}N_{i,j}\beta_{i,j}+1}+\mathcal{O}\left(\frac{1}{s^{M_{i,j}N_{i,j}\beta_{i,j}+2}}\right)\right] \tag{38}$$

which can be written under the form:

$$\mathcal{M}_{\mathcal{I}_{\mathcal{S},j}}(s)=\left[\prod_{i\in\mathcal{S}}C_{i,j}^{M_{i,j}N_{i,j}}\right]\left[\frac{c_0}{s^\tau}+\frac{c_1}{s^{\tau+1}}+\mathcal{O}\left(\frac{1}{s^{\tau+2}}\right)\right] \tag{39}$$

where:

$$\tau=\sum_{i\in\mathcal{S}}M_{i,j}N_{i,j}\beta_{i,j} \tag{40}$$

$$c_0=\prod_{i\in\mathcal{S}}\left(\frac{M_{i,j}}{G_{i,j}r_{i,j}A_{i,j}}\right)^{M_{i,j}N_{i,j}\beta_{i,j}} \tag{41}$$

The term c_1 is given by:

$$c_1=-\sum_{i\in\mathcal{S}}M_{i,j}N_{i,j}\beta_{i,j}\left(\frac{M_{i,j}}{G_{i,j}r_{i,j}A_{i,j}}\right)^{M_{i,j}N_{i,j}\beta_{i,j}+1}\prod_{\substack{i'\in\mathcal{S}\\ i'\neq i}}\left(\frac{M_{i',j}}{G_{i',j}r_{i',j}A_{i',j}}\right)^{M_{i',j}N_{i',j}\beta_{i',j}} \tag{42}$$

which, after straightforward manipulations, can be written as:

$$c_1=-c_0\sum_{i\in\mathcal{S}}\left(\frac{M_{i,j}^2N_{i,j}\beta_{i,j}}{G_{i,j}r_{i,j}A_{i,j}}\right) \tag{43}$$

Based on (39) and proposition-1 in [18], the pdf of $\mathcal{I}_{\mathcal{S},j}$ can be approximated by: $\left[\prod_{i\in\mathcal{S}}C_{i,j}^{M_{i,j}N_{i,j}}\right]\frac{c_0}{\Gamma(\tau)}I^{\tau-1}e^{\frac{c_1}{c_0\tau}I}$ which after straightforward manipulations can be written as:

$$f_{\mathcal{I}_{\mathcal{S},j}}(I)=K_{\mathcal{S},j}f_\gamma\left(I,\tau_{\mathcal{S},j},\Lambda_{\mathcal{S},j}\right) \tag{44}$$

where $\tau_{\mathcal{S},j}=\tau$ which from (40) results in:

$$\tau_{\mathcal{S},j}=\sum_{i\in\mathcal{S}} M_{i,j}N_{i,j}\beta_{i,j} \tag{45}$$

and where $\Lambda_{\mathcal{S},j}=-\frac{c_0\tau}{c_1}$ which from (40) and (43) results in:

$$\Lambda_{\mathcal{S},j}=\frac{\sum_{i\in\mathcal{S}} M_{i,j}N_{i,j}\beta_{i,j}}{\sum_{i\in\mathcal{S}}\frac{M_{i,j}^2N_{i,j}\beta_{i,j}}{G_{i,j}r_{i,j}A_{i,j}}} \tag{46}$$

and where $K_{\mathcal{S},j}=\left[\prod_{i\in\mathcal{S}} C_{i,j}^{M_{i,j}N_{i,j}}\right]c_0\Lambda_{\mathcal{S},j}^{\tau_{\mathcal{S},j}}$ which from (41), (45) and (46) can be written as:

$$K_{\mathcal{S},j}=\Lambda_{\mathcal{S},j}^{\tau_{\mathcal{S},j}}\prod_{i\in\mathcal{S}}\left(\frac{C_{i,j}^{1/\beta_{i,j}}M_{i,j}}{G_{i,j}r_{i,j}A_{i,j}}\right)^{M_{i,j}N_{i,j}\beta_{i,j}} \tag{47}$$

From (34), the outage probability of the multi-source transmissions from nodes in $\mathcal{S}$ towards R_j can be written as:

$$p_{\mathcal{S},j}\triangleq\Pr\left(\gamma_{\mathcal{S},j}<\gamma_{th}\right)=\Pr\left(\mathcal{I}_{\mathcal{S},j}<\left[\frac{P_M}{\sqrt{\sum_{i\in\mathcal{S}}N_{i,j}}}\right]^{-1}\right) \tag{48}$$

which, from (44), can be approximated by:

$$p_{\mathcal{S},j}=\frac{K_{\mathcal{S},j}}{\Gamma(\tau_{\mathcal{S},j})}\gamma\left(\tau_{\mathcal{S},j},\left[\frac{\Lambda_{\mathcal{S},j}P_M}{\sqrt{\sum_{i\in\mathcal{S}}N_{i,j}}}\right]^{-1}\right) \tag{49}$$

which tends to $\frac{K_{\mathcal{S},j}}{\Gamma(\tau_{\mathcal{S},j}+1)}\Lambda_{\mathcal{S},j}^{-\tau_{\mathcal{S},j}}\left[\frac{P_M}{\sqrt{\sum_{i\in\mathcal{S}}N_{i,j}}}\right]^{-\tau_{\mathcal{S},j}}$ for large values of P_M. Invoking (15), (16), (45) and (47):

$$p_{\mathcal{S},j}=\left[\prod_{i\in\mathcal{S}}\left(\frac{\Gamma(\alpha_{i,j}-\beta_{i,j})}{\Gamma(\alpha_{i,j})}\left[\frac{M_{i,j}\alpha_{i,j}\beta_{i,j}}{G_{i,j}r_{i,j}}\right]^{\beta_{i,j}}\right)^{M_{i,j}N_{i,j}}\right]\frac{1}{\Gamma\left(\sum_{i\in\mathcal{S}}M_{i,j}N_{i,j}\beta_{i,j}+1\right)}\left(\frac{P_M}{\sqrt{\sum_{i\in\mathcal{S}}N_{i,j}}}\right)^{-\sum_{i\in\mathcal{S}}M_{i,j}N_{i,j}\beta_{i,j}} \tag{50}$$

which reduces to (24) for $|\mathcal{S}|=1$.

Equation (50) shows that the diversity gain in the case of multi-source transmissions is equal to the sum of the diversity gains achieved by each of the transmitting sources. In particular, the diversity gain of the transmissions from $\{\mathrm{R}_i\}_{i\in\mathcal{S}}$ to R_j is $\sum_{i\in\mathcal{S}}M_{i,j}N_{i,j}\beta_{i,j}$.

IV. Performance Analysis of Cooperative Systems

A. All-Active Relaying

For all-active relaying, the transmit power is evenly split among the $2N_r+1$ S-D, S-R and R-D links that are all activated. In this case, $r_{i,j}$ is set to $\frac{1}{2N_r+1}$ in the outage probability expressions of the constituent SISO, MIMO, or MS links in (17)-(19), (23)-(24) and (49)-(50), respectively. Note that for MIMO all-active relaying, RC is applied at the intermediate links and the resulting system can be implemented in the absence of CSI and feedback. The outage probability of all-active parallel-relaying FSO systems with SISO links over lognormal channels was first derived in [12]. In particular, equation (31) in [12] can be written under the following form that is more amenable to a diversity gain analysis with MIMO links over gamma-gamma fading channels:

$$P_{out}=\sum_{i=0}^{N_r}\sum_{j=1}^{\binom{N_r}{i}}\left[\prod_{k\in\mathcal{I}_{i,j}}p_{0,k}\prod_{k'\in\overline{\mathcal{I}}_{i,j}}(1-p_{0,k'})\right]p_{\left\{\{0\}\cup\overline{\mathcal{I}}_{i,j}\right\},N_r+1} \tag{51}$$

where i corresponds to the number of relays that are in outage. $\mathcal{I}_{i,1},\ldots,\mathcal{I}_{i,\binom{N_r}{i}}$ are all possible subsets of $\{1,\ldots,N_r\}$ having i elements each while $\overline{\mathcal{I}}_{i,j}=\{1,\ldots,N_r\}\backslash\mathcal{I}_{i,j}$. The term inside the double summation in (51) corresponds to the case where the relays in $\mathcal{I}_{i,j}$ are in outage while the remaining relays (in $\overline{\mathcal{I}}_{i,j}$) are not in outage; in this case, relays in $\overline{\mathcal{I}}_{i,j}$ as well as the source node will transmit simultaneously to D and the corresponding outage probability would be $p_{\left\{\{0\}\cup\overline{\mathcal{I}}_{i,j}\right\},N_r+1}$ whose general form is given in (49). Outage probabilities of the form $p_{0,k}$ in (51) are provided in (17) and (23) in the cases of SISO and MIMO links, respectively.

Proposition *1:* The diversity gain achieved by all-active relaying over gamma-gamma fading channels is:

$$\nu=M_{0,N_r+1}N_{0,N_r+1}\beta_{0,N_r+1}+\sum_{n=1}^{N_r}\min\{M_{0,n}N_{0,n}\beta_{0,n},M_{n,N_r+1}N_{n,N_r+1}\beta_{n,N_r+1}\} \tag{52}$$

Proof: The proof is provided in appendix A. ■

Approximating (51) by the term that scales asymptotically as $P_M^{-\nu}$ results in:

$$P_{out}\approx\left[\prod_{n\in\mathbb{V}(D)}p_{0,n}\right]p_{\{\{0\}\cup\mathbb{V}(S)\},N_r+1} \tag{53}$$

where $\mathbb{V}(D)$ (resp. $\mathbb{V}(S)$) stands for the set of relays R_n for which $M_{0,n}N_{0,n}\beta_{0,n}$ is less (resp. greater) than $M_{n,N_r+1}N_{n,N_r+1}\beta_{n,N_r+1}$. For SISO links (or MIMO links in the case where the product $M_{i,j}N_{i,j}$ is constant), $\mathbb{V}(S)$ and $\mathbb{V}(D)$ stand for the set of relays in the vicinity of S and D, respectively, since the channel parameter β is a decreasing function of the link distance.

B. Selective Relaying

In selective relaying, the information symbols are transmitted along the strongest path among the N_r+1 paths S-D, S-R_1-D, ... , S-R_{N_r}-D where along each constituent link the transmit aperture ensuring the highest path gain is activated (TLS scheme). In this case, D is in outage when the above N_r+1 paths all suffer from outage resulting in:

$$P_{out}=p_{0,N_r+1}\prod_{n=1}^{N_r}\left[p_{0,n}+p_{n,N_r+1}-p_{0,n}p_{n,N_r+1}\right] \tag{54}$$

where the term inside the product follows since S-R_n-D is not in outage when both links S-R_n and R_n-D are not in outage; that is, with probability $(1-p_{0,n})(1-p_{n,N_r+1})$. The outage probabilities of the form $p_{i,j}$ in (54) are provided in (17) and (29) in the cases of SISO and MIMO links, respectively. Note that for selective relaying, multi-source transmissions do not occur since, for a ceratin channel realization, only one node

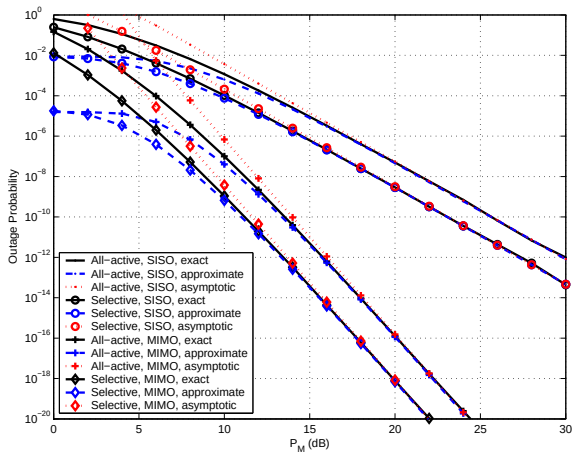

Fig. 5. Performance with 1 relay for $d_{SD} = 3$ km.

(whether S or a relay) is transmitting towards D. For the single-hop path S-D, we set $r_{0,N_r+1} = 1$ in (17) and (29) for the evaluation of p_{0,N_r+1}. For the two-hop path S-R$_n$-D, we set $r_{0,n} = r_{n,N_r+1} = \frac{1}{2}$ for the evaluation of $p_{0,n}$ and p_{n,N_r+1}.

Following from the asymptotic expression of $p_{i,j}$ in (30) that scales asymptotically as $P_M^{-M_{i,j}N_{i,j}\beta_{i,j}}$ (and that comprises SISO links as a special case), (54) shows that the diversity gain achieved by selective relaying is as in (52). In other words, the diversity gain achieved by a cooperative FSO network is the same whether selective relaying or all-active relaying (with diversity combining at D) is implemented [1]. This constitutes one of the findings of the paper that was not reported previously in the literature. Despite the fact that all-active relaying, that is based on evenly distributing the power among the FSO links, is far from being optimal especially when the distances of the links are remarkably different, this simple scheme that can be implemented in the absence of CSI is capable of achieving the same diversity gain as the more complicated selective-relaying scheme.

Note that the optimal power allocation strategy (PAS) in the case of parallel-relaying corresponds to selecting the "best" S-R-D link and optimally allocating the power among the two hops of this link [16]. Consequently, the difference between the optimal PAS and the considered selective-relaying scheme resides in adapting the values of $r_{0,n}$ and r_{n,N_r+1} to the strengths of the two hops rather than setting $r_{0,n} = r_{n,N_r+1} = \frac{1}{2}$ as in (54). However, from [16], the optimal PAS does not change the diversity gain. Consequently, the presented comparison between MIMO and relay-assisted systems holds in the case of the optimal PAS as well since this comparison is based on the achievable diversity gains.

For asymptotic values of P_M, (54) can be approximated by the term that scales as $P_M^{-\nu}$ resulting in:

$$P_{out} \approx p_{0,N_r+1} \left[\prod_{n\in\mathbb{V}(D)} p_{0,n} \right] \left[\prod_{n\in\mathbb{V}(S)} p_{n,N_r+1} \right] \quad (55)$$

[1]Note that for all-active relaying with the switching scheme [9]–[11], the outage probability takes the form in (54) and (55) where $r_{i,j}$ needs to be replaced by $\frac{1}{2N_r+1}$. Consequently, [9]–[11] achieve the same diversity gain as selective relaying and all-active relaying with diversity combining.

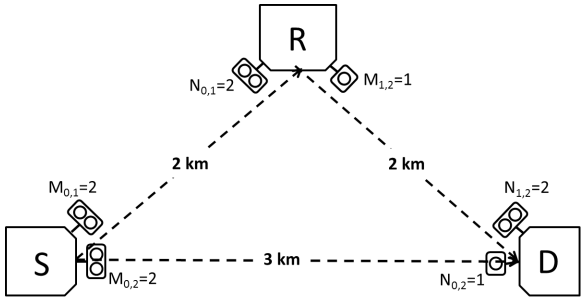

Fig. 6. The simulation setup of Fig. 5.

C. Coding Gain

The asymptotic values of $p_{0,n}$ and $p_{\{\{0\}\cup\mathbb{V}(S)\},N_r+1}$ in (53) are given in (24) and (50) while the asymptotic values of $p_{0,n}$ and p_{n,N_r+1} in (55) are given in (30). Moreover, (53) and (55) differ by the value of $r_{i,j}$ that is equal to $\frac{1}{2N_r+1}$ for all-active relaying and to 1 or $\frac{1}{2}$ for selective relaying.

Replacing (24) and (50) in (53) and (30) in (55), and after straightforward calculations, we can prove that the advantage of selective relaying compared to all-active relaying resides in a coding gain given in (56) shown at the top of the next page. In (56), $\nu_{i,j} \triangleq M_{i,j}N_{i,j}\beta_{i,j}$ while ν is the diversity gain given in (52). The coding gain in (56) stems out from the following, (i): the transmit laser selection protocol implemented at each link, (ii): the relay selection protocol that ensures that the best path is selected and (iii): the fact that the power is spread over a smaller number of links (one or two links for selective relaying versus $2N_r + 1$ links for all-active relaying).

In the case of SISO links, which constitutes the case that has been considered so far in the literature, (56) reduces to:

$$\frac{10}{\nu}\log_{10}\left[2^{\beta_{0,N_r+1}}\left(\frac{2N_r+1}{2}\right)^{\nu}\frac{\sqrt{|\mathbb{V}'(S)|}^{\sum_{n\in\mathbb{V}'(S)}\beta_{n,N_r+1}}}{\Gamma(\sum_{n\in\mathbb{V}'(S)}\beta_{n,N_r+1}+1)}\left(\prod_{n\in\mathbb{V}'(S)}\Gamma(\beta_{n,N_r+1}+1)\right)\right] \quad (57)$$

where $\mathbb{V}'(S) \triangleq \{0\} \cup \mathbb{V}(S)$. Equations (56) and (57) are additional contributions of the paper and they directly link the coding advantage of selective relaying (over all-active relaying) to the topology of the FSO network.

Fig. 5 shows the performance with one relay for $d_{SD} = 3$ km and $d_{SR} = d_{RD} = 1.5$ km. For the case of MIMO-relays, the S-D link is a 2×1 link ($M_{0,2} = 2$ and $N_{0,2} = 1$), the S-R link is a 2×2 link ($M_{0,1} = N_{0,1} = 2$) and the R-D link is a 1×2 link ($M_{1,2} = 1$ and $N_{1,2} = 2$). The simulation setup is better illustrated in Fig. 6. Results show the accuracy of the approximate expressions in determining the performance for average-to-large values of P_M as well as the accuracy of the asymptotic expressions for predicting the diversity gains and coding gains. As expected, selective relaying and all-active relaying achieve the same diversity gains where the corresponding outage curves are parallel for large values of P_M. The superiority of selective relaying is also evident whether with SISO or MIMO links.

$$\frac{10}{\nu}\log_{10}\left[2^{\nu_{0,N_r+1}}\left(\frac{2N_r+1}{2}\right)^{\nu}\frac{\sqrt{\sum_{n\in\{0\}\cup\mathbb{V}(S)}N_{n,N_r+1}}^{\sum_{n\in\{0\}\cup\mathbb{V}(S)}\nu_{n,N_r+1}}}{\Gamma(\sum_{n\in\{0\}\cup\mathbb{V}(S)}\nu_{n,N_r+1}+1)}\left(\prod_{n\in\mathbb{V}(D)}\frac{M_{0,n}^{\nu_{0,n}}\Gamma(N_{0,n}\beta_{0,n}+1)^{M_{0,n}}}{\Gamma(\nu_{0,n}+1)}\right)\right.$$
$$\left.\left(\prod_{n\in\{0\}\cup\mathbb{V}(S)}\Gamma(N_{n,N_r+1}\beta_{n,N_r+1}+1)^{M_{n,N_r+1}}\left(\frac{M_{n,N_r+1}}{\sqrt{N_{n,N_r+1}}}\right)^{\nu_{n,N_r+1}}\right)\right] \quad (56)$$

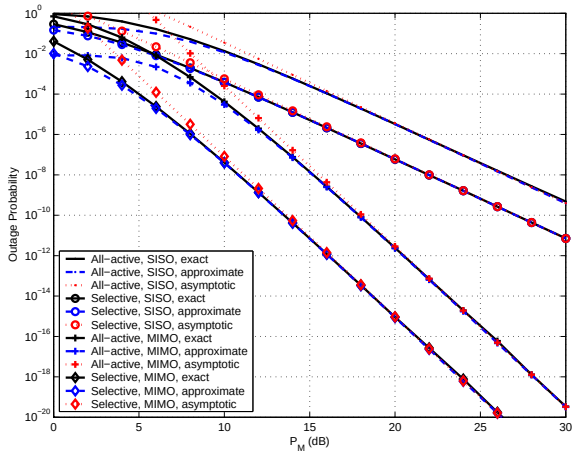

Fig. 7. Performance with 2 relays for $d_{SD} = 5$ km.

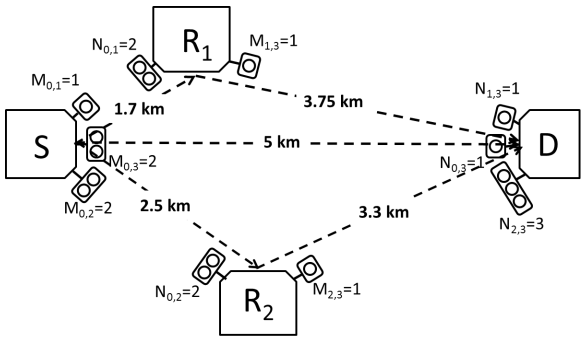

Fig. 8. The simulation setup of Fig. 7.

Fig. 7 shows the performance with two relays for $d_{SD} = 5$ km, $(d_{SR_1}, d_{R_1D}) = (1.7, 3.75)$ km and $(d_{SR_2}, d_{R_2D}) = (2.5, 3.3)$ km. For the case of MIMO-relays, the S-D link is a 2×1 link ($M_{0,3} = 2$ and $N_{0,3} = 1$), the S-R_1 link is a 1×2 link ($M_{0,1} = 1$ and $N_{0,1} = 2$), the S-R_2 link is a 2×2 link ($M_{0,2} = N_{0,2} = 2$), the R_1-D link is a 1×1 link ($M_{1,3} = N_{1,3} = 1$) and the R_2-D link is a 1×3 link ($M_{2,3} = 1$ and $N_{2,3} = 3$). The simulation setup is better illustrated in Fig. 8. Results show the enhanced accuracy of the derived expressions for such longer distances. (56) and (57) accurately predict coding gains of 4.38 dB and 4.47 dB for MIMO and SISO links, respectively.

V. Optimizing the Number of Apertures

In this section, we compare the diversity gains of cooperative systems and MIMO systems under the constraint that the total number of apertures is the same. For simplicity, we consider the case where the number of transmit and receive apertures along each intermediate FSO link is the same; that is, $M_{i,j} = N_{i,j}$ for all values of i and j.

From (52), the diversity gain achieved by cooperative systems (whether with the all-active or selective schemes) is:

$$\nu_R = N_{0,N_r+1}^2\beta_{0,N_r+1} + \sum_{n=1}^{N_r}\min\{N_{0,n}^2\beta_{0,n}, N_{n,N_r+1}^2\beta_{n,N_r+1}\} \quad (58)$$

The above diversity gain will be compared with that of a MIMO system (whether with RC or TLS) where all the transmit apertures will be placed at S and the receive apertures at D. In other words, the MIMO system is a $N_{tot} \times N_{tot}$ system where $N_{tot} = N_{0,N_r+1} + \sum_{n=1}^{N_r}(N_{0,n} + N_{n,N_r+1})$. From the performance analysis of MIMO systems in subsection III-B, the diversity gain of the MIMO system is:

$$\nu_{MIMO} = \left[N_{0,N_r+1} + \sum_{n=1}^{N_r}(N_{0,n} + N_{n,N_r+1})\right]^2 \beta_{0,N_r+1} \quad (59)$$

Proposition *2:* ν_{MIMO} in (59) is greater than ν_R in (58) for all values of N_{0,N_r+1} and $\{N_{0,n}, N_{n,N_r+1}\}_{n=1}^{N_r}$ and for all values of β_{0,N_r+1} and $\{\beta_{0,n}, \beta_{n,N_r+1}\}_{n=1}^{N_r}$ satisfying (4).

Proof: The proof is provided in appendix B. ■

For example, in Fig. 5, the SISO and MIMO cooperative networks achieve the diversity gains of 3.79 and 7.58, respectively, whereas the equivalent 3×3 and 5×5 MIMO systems achieve the diversity gains of 13.77 and 38.26, respectively.

Finally, note that while proposition 2 holds in the case of independent fading, future work needs to target the impact of correlation between the multiple apertures of the same node.

VI. Effect of Aperture Averaging

All of the previously presented calculations and results hold in the case of point receivers where the receiver lens diameter (denoted by D in what follows) is equal to zero. In particular, the expressions of the channel parameters α and β in (3)-(4) as well as the power series expansion in (12)-(13) hold in this special case of $D = 0$. For receivers that implement aperture averaging, $D > 0$ resulting in a decrease of the variance of intensity fluctuations. In this case, the gamma-gamma statistical model can still be used but with modified parameters α and β [21], [22].

The impact of aperture averaging on the presented calculations is that (12)-(13) do not hold anymore since for $D > 0$ the parameter β can be greater than the parameter α unlike the case of point receivers. However, this can be easily remedied since in the case of $\beta > \alpha$, (12)-(13) can be written as $f_{\gamma\gamma}(I) \approx a_0 I^{\alpha-1} + a_1 I^{\alpha}$ where, in this case,

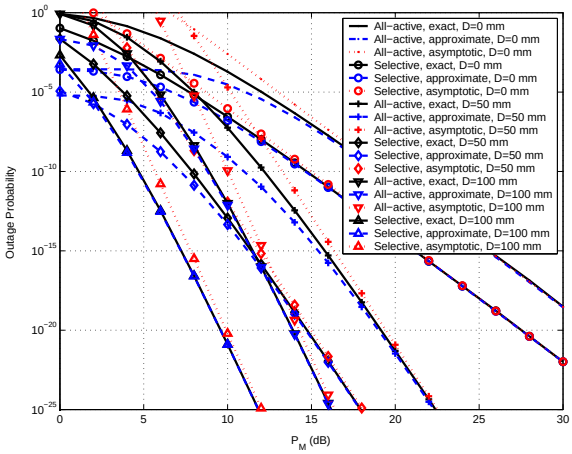

Fig. 9. Effect of aperture averaging on the performance with 2 relays for $d_{SD} = 3$ km.

$a_0 = \frac{\Gamma(\beta-\alpha)}{\Gamma(\alpha)\Gamma(\beta)}(\alpha\beta)^{\alpha}$ and $a_1 = \frac{\Gamma(\beta-\alpha)}{\Gamma(\alpha)\Gamma(\beta)}\frac{(\alpha\beta)^{\alpha+1}}{(1-\beta+\alpha)}$. These expressions are similar to (12)-(13) where the roles of α and β need to be interchanged when $\beta > \alpha$. As a conclusion, all of the derived outage probability expressions, diversity gains and coding gains will still hold by replacing β with $\min(\alpha, \beta)$ and α with $\max(\alpha, \beta)$.

Fig. 9 shows the performance with two relays for $d_{SD} = 3$ km, $d_{SR_1} = d_{R_1D} = 1.5$ km and $d_{SR_2} = d_{R_2D} = 1.55$ km in the case of SISO-relays. The lens diameter D is varied between 0 mm and 100 mm and a zero inner scale of turbulence is assumed. Results show the accuracy of the derived outage probability expressions. In particular, the gap between the exact and approximate expressions is reduced for increasing values of D. Finally, as in the case of point receivers, all-active relaying and selective relaying achieve the same diversity gain.

Regarding the comparison between MIMO and relay-assisted systems, the result in proposition 2 that shows the superiority of MIMO techniques for all network configurations follows mainly from the relation given in (77) in appendix B. While (77) holds for all link distances and values of C_n^2 in the case of point receivers ($D = 0$), this relation does not always hold when aperture averaging is performed ($D > 0$). In this case, the superiority of one diversity technique over the other depends on the specific topology of the network.

Defining $\mathcal{D} = \{d_{0,n}, d_{n,N_r+1}\}_{n=1}^{N_r}$ as the set of all source-relay and relay-destination distances, and following from the proof in appendix B, MIMO techniques will be superior to cooperative techniques if all distances d in $\mathcal{D}$ satisfy the following relation:

$$\left[\frac{\beta(d')}{\beta(d_{SD})}\right]^{-1/2} \geq \frac{d'}{d_{SD}} \quad ; \quad d' = d, (d_{SD} - d) \tag{60}$$

and, on the other hand, if not all distances in $\mathcal{D}$ satisfy (60), then MIMO techniques may or may not achieve higher diversity gains than cooperative techniques depending on the specific network topology.

We define $\mathcal{I}$ as the subinterval of $[0 \quad d_{SD}]$ for which (60) is satisfied (MIMO is always superior). The size of $\mathcal{I}$ increases when the turbulence-induced fading becomes stronger; that is, for larger values of C_n^2, longer source-destination distances and smaller values of D. As an extreme case, for $D = 0$, $\mathcal{I} = [0 \quad d_{SD}]$ and, consequently, $\mathcal{D}$ is always included in $\mathcal{I}$ highlighting the unconditional superiority of MIMO techniques for all network configurations in this case. As an example, for $d_{SD} = 3$ km, $\mathcal{I} = [0.77 \quad 2.23]$ (km) for $C_n^2 = 1.7 \times 10^{-15}$ m$^{-2/3}$ and $D = 50$ mm. This interval reduces to the empty interval when increasing D above 100 mm (while keeping the same value of C_n^2) and it extends over the entire interval $[0 \quad 3]$ (km) (meaning that MIMO is always better) when increasing C_n^2 above 1.7×10^{-13} m$^{-2/3}$ (while keeping the same value of D). On the other hand, for $d_{SD} = 10$ km, $\mathcal{I} = [0.1 \quad 9.9]$ (km) for $C_n^2 = 1.7 \times 10^{-15}$ m$^{-2/3}$ and $D = 50$ mm. In a similar way, MIMO techniques are always superior to cooperative techniques for source-destination distances exceeding 3 km for all values of D and for large values of C_n^2 exceeding 1.7×10^{-13} m$^{-2/3}$.

For the simulation setup of Fig. 9, $\mathcal{I}$ takes the values of $[0.075 \quad 2.925]$ (km) and $[0.348 \quad 2.652]$ (km) for $D = 50$ mm and $D = 100$ mm, respectively. Given that the distances $d_{SR_1} = d_{R_1D} = 1.5$ km and $d_{SR_2} = d_{R_2D} = 1.55$ km fall in both intervals, then MIMO systems are superior to relay-assisted systems for this simulation setup. In particular, $\nu_{MIMO} = 13.77$ and $\nu_R = 7.97$ for $D = 0$ mm, $\nu_{MIMO} = 38$ and $\nu_R = 16.21$ for $D = 50$ mm and $\nu_{MIMO} = 42.98$ and $\nu_R = 23.55$ for $D = 100$ mm.

As a conclusion, the above analysis highlights the interest of MIMO systems over long communication distances and/or under strong atmospheric turbulence and/or for receivers that implement limited levels of aperture averaging. Note that in the case where the relays are placed midway between S and D, the distances in $\mathcal{D}$ have higher probabilities to fall within the interval $\mathcal{I}$ that is always centered at $d_{SD}/2$ thus highlighting the advantage of MIMO systems in this scenario as well.

VII. Conclusion

For point receivers, adding relays for the purpose of assisting a couple of FSO nodes in their communication is not useful since an equivalent MIMO system deploying the same total number of transmit and receive apertures is capable of achieving a higher diversity gain. In other words, to upgrade an existing FSO network for combatting fading, it is better to invest in adding more apertures to the communicating nodes rather than adding more relays in their vicinity. This follows from the non-broadcast nature of FSO transmissions where the communication between a relay with S and D requires two separate transceivers. This does not mean that cooperation is not useful for FSO systems. Nevertheless, cooperation must be realized with existing nodes (that will serve as relays) where this operation mode does not require any additional infrastructure and where taking advantage of the presence of the neighboring nodes constitutes an additional degree of freedom that is incontestably beneficial. In the case where aperture averaging is performed at the relays and destination, MIMO techniques maintain their superiority over cooperative techniques for all network configurations under strong

turbulence. In the cases of weak to average turbulence, the superiority of one diversity technique over the other depends on the specific topology of the network. While the findings of this paper are limited to the case of independent fading, future work must consider the impact of channel correlation on the achievable diversity gains and on the superiority of one diversity method over the other.

APPENDIX A

The probability $p_{0,k}$ in (51) scales asymptotically as $P_M^{-\nu_{0,k}}$ from (19) and (24) where $\nu_{i,j} \triangleq M_{i,j}N_{i,j}\beta_{i,j}$. On the other hand, $p_{\left\{\{0\}\cup\overline{\mathcal{I}}_{i,j}\right\},N_r+1}$ scales asymptotically as $P_M^{-\sum_{k\in\{\{0\}\cup\overline{\mathcal{I}}_{i,j}\}}\nu_{k,N_r+1}}$ from (50). Consequently, the diversity gain of (51) is given by:

$$\nu=\nu_{0,N_r+1}+\min_{\substack{i=0,\ldots,N_r\\ j=1,\ldots,\binom{N_r}{i}}}\left\{\sum_{k_1\in\mathcal{I}_{i,j}}\nu_{0,k_1}+\sum_{k_2\in\overline{\mathcal{I}}_{i,j}}\nu_{k_2,N_r+1}\right\} \quad (61)$$

Adding and subtracting the term $\sum_{k_2\in\mathcal{I}_{i,j}}\nu_{k_2,N_r+1}$ inside the double minimization in (61), and since $\sum_{k_2\in\mathcal{I}_{i,j}}\nu_{k_2,N_r+1}+\sum_{k_2\in\overline{\mathcal{I}}_{i,j}}\nu_{k_2,N_r+1}=\sum_{k_2=1}^{N_r}\nu_{k_2,N_r+1}$ is independent of i and j, then (61) can be written as:

$$\nu=\sum_{k=0}^{N_r}\nu_{k,N_r+1}+\min_{\substack{i=0,\ldots,N_r\\ j=1,\ldots,\binom{N_r}{i}}}\left\{\sum_{k\in\mathcal{I}_{i,j}}(\nu_{0,k}-\nu_{k,N_r+1})\right\} \quad (62)$$

The minimization for $i=0,\ldots,N_r$ and $j=1,\ldots,\binom{N_r}{i}$ is equivalent to the minimization over all possible subsets of $\{1,\ldots,N_r\}$ and (62) can be written as:

$$\nu=\sum_{k=0}^{N_r}\nu_{k,N_r+1}+\min_{\mathcal{S}\subset\{1,\ldots,N_r\}}\{\nu_{\mathcal{S}}\} \quad (63)$$

where $\nu_{\mathcal{S}}\triangleq\sum_{k\in\mathcal{S}}(\nu_{0,k}-\nu_{k,N_r+1})$.

We will next prove that the minimum value of $\nu_{\mathcal{S}}$ is attained by the set $\mathcal{N}=\{n\mid\nu_{0,n}\le\nu_{n,N_r+1}\}$. The following cases are possible. (i): $\mathcal{S}=\varphi$. In this case, $\nu_{\mathcal{S}}=0$ while $\nu_{\mathcal{N}}\le 0$ since it corresponds to the summation of $|\mathcal{N}|$ terms that are either zero or negative. (ii): $\mathcal{S}\subset\mathcal{N}$. In this case, $\nu_{\mathcal{N}}$ can be written as $\nu_{\mathcal{N}}=\nu_{\mathcal{S}}+\nu_{\mathcal{N}\backslash\mathcal{S}}$ implying that $\nu_{\mathcal{N}}\le\nu_{\mathcal{S}}$ since $\nu_{\mathcal{N}\backslash\mathcal{S}}$ (over a subset of $\mathcal{N}$) is negative or zero. (iii): $\mathcal{S}\subset\{1,\ldots,N_r\}\backslash\mathcal{N}$. In this case, $\nu_{\mathcal{S}}\ge 0$ while $\nu_{\mathcal{N}}\le 0$ implying that $\nu_{\mathcal{N}}\le\nu_{\mathcal{S}}$. (iv): $\mathcal{S}=\mathcal{S}_1\cup\mathcal{S}_2$ where $\mathcal{S}_1\subset\mathcal{N}$ while $\mathcal{S}_2\subset\{1,\ldots,N_r\}\backslash\mathcal{N}$. In this case, $\nu_{\mathcal{S}}=\nu_{\mathcal{S}_1}+\nu_{\mathcal{S}_2}$ where $\nu_{\mathcal{S}_1}\ge\nu_{\mathcal{N}}$ from case (ii) and $\nu_{\mathcal{S}_2}\ge\nu_{\mathcal{N}}$ from case (iii) implying that $\nu_{\mathcal{S}}\ge\nu_{\mathcal{N}}$. Therefore, in all cases, $\nu_{\mathcal{N}}\le\nu_{\mathcal{S}}$ and $\min_{\mathcal{S}\subset\{1,\ldots,N_r\}}\{\nu_{\mathcal{S}}\}=\nu_{\mathcal{N}}$ and (63) simplifies to:

$$\nu=\sum_{k=0}^{N_r}\nu_{k,N_r+1}+\sum_{\substack{k=1\\ \nu_{0,k}\le\nu_{k,N_r+1}}}^{N_r}(\nu_{0,k}-\nu_{k,N_r+1}) \quad (64)$$

Equation (64) can be written as:

$$\nu=\sum_{k=0}^{N_r}\nu_{k,N_r+1}+\sum_{k=1}^{N_r}\min\{0,\nu_{0,k}-\nu_{k,N_r+1}\} \quad (65)$$

$$=\nu_{0,N_r+1}+\sum_{k=1}^{N_r}(\nu_{k,N_r+1}+\min\{0,\nu_{0,k}-\nu_{k,N_r+1}\}) \quad (66)$$

The term inside the summation of (66) can be written as $\min\{\nu_{k,N_r+1},\nu_{0,k}\}$ completing the proof of proposition 1.

APPENDIX B

Equation (59) can be lower-bounded by:

$$\nu_{MIMO}>\left[N_{0,N_r+1}^2+\sum_{n=1}^{N_r}(N_{0,n}+N_{n,N_r+1})^2\right]\beta_{0,N_r+1} \quad (67)$$

$$=\left[N_{0,N_r+1}^2+\sum_{n=1}^{N_r}(N_{n,min}+N_{n,max})^2\right]\beta_{0,N_r+1} \quad (68)$$

where the inequality in (67) is strict since the number of apertures is nonzero. In (68), $N_{n,min}\triangleq\min\{N_{0,n},N_{n,N_r+1}\}$ and $N_{n,max}\triangleq\max\{N_{0,n},N_{n,N_r+1}\}$.

In an attempt to upper-bound (58), the cooperative network will be compared with a second hypothetical network. The positions of the relays in this second network are obtained from projecting the positions of the relays of the first network along S-D. Denoting the relays of the hypothetical network by R'$_1,\ldots,$R'$_{N_r}$ where each relay is placed at the projected position, then $d_{S,R'_n}\le d_{S,R_n}$ and $d_{R'_n,D}\le d_{R_n,D}$ for all values of n. Consequently, $\beta_{0,n}\le\beta'_{0,n}=\beta(d_{S,R'_n})$ and $\beta_{n,N_r+1}\le\beta'_{n,N_r+1}=\beta(d_{R'_n,D})$ where, from (4), β' stands for the parameter of the channel at the projected relay position. Therefore, (58) can be upper-bounded as:

$$\nu_R\le N_{0,N_r+1}^2\beta_{0,N_r+1}+\sum_{n=1}^{N_r}\min\{N_{0,n}^2\beta'_{0,n},N_{n,N_r+1}^2\beta'_{n,N_r+1}\} \quad (69)$$

$$\le N_{0,N_r+1}^2\beta_{0,N_r+1}+\sum_{n=1}^{N_r}N_{n,max}^2\beta'_{n,mim} \quad (70)$$

where $\beta'_{n,min}\triangleq\min\{\beta'_{0,n},\beta'_{n,N_r+1}\}$ and $\beta'_{n,max}\triangleq\max\{\beta'_{0,n},\beta'_{n,N_r+1}\}$. Equation (70) follows since $N_{0,n}\le N_{n,max}$ and $N_{n,N_r+1}\le N_{n,max}$.

On the other hand, given that the minimum of two functions is maximized at one of their points of intersection, then the ultimate maximum (for integer and non-integer values of $N_{0,n}$ and N_{n,N_r+1}) of the minimization in (69) is achieved for the not-necessarily integer values of $N_{0,n}$ and N_{n,N_r+1} satisfying:

$$N_{0,n}^2\beta'_{0,n}=N_{n,N_r+1}^2\beta'_{n,N_r+1} \quad (71)$$

In other words, the value of $\min\{N_{0,n}^2\beta'_{0,n},N_{n,N_r+1}^2\beta'_{n,N_r+1}\}$ achieved for integer values of $N_{0,n}$ and N_{n,N_r+1} would be less than the value achieved for the values of $N_{0,n}$ and N_{n,N_r+1} satisfying (71).

From (71), if $\beta'_{0,n}$ is less than β'_{n,N_r+1}, then $N_{0,n}$ will be greater than N_{n,N_r+1} and vice versa. Consequently, (71) can be written as:

$$N_{n,max}^2\beta'_{n,min}=N_{n,min}^2\beta'_{n,max} \quad (72)$$

Subtracting (70) from (68) and applying the relation in (72):

$$\nu_{MIMO}-\nu_R>\beta_{0,N_r+1}\sum_{n=1}^{N_r}N_{n,max}^2\Delta_n \quad (73)$$

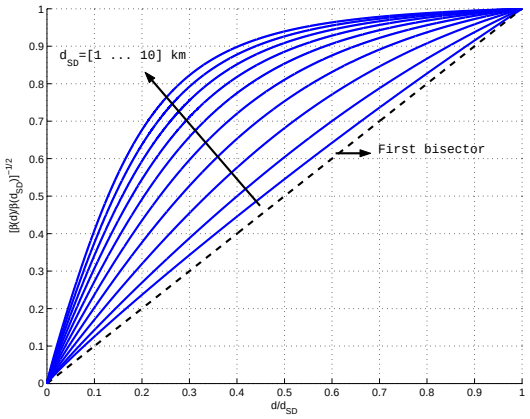

Fig. 10. The function $[\beta(d)/\beta(d_{SD})]^{-\frac{1}{2}}$ vs. the normalized distance d/d_{SD}.

where:

$$\Delta_n = \left[1 + \sqrt{\frac{\beta'_{n,min}}{\beta'_{n,max}}}\right]^2 - \frac{\beta'_{n,min}}{\beta_{0,N_r+1}} \tag{74}$$

We will next prove that $\Delta_n \geq 0$. Given that $\beta'_{n,min}$ and $\beta'_{n,max}$ are the channel parameters of a hypothetical relay along S-D, then these quantities can be written, from (4), as:

$$\beta'_{n,max} = \beta(d) \;\; , \;\; \beta'_{n,min} = \beta(d_{SD} - d) \;\; ; \;\; d \leq \frac{1}{2} d_{SD} \tag{75}$$

where $\beta'_{n,max}$ and $\beta'_{n,min}$ are associated with the minimum and maximum distances, respectively.

Following from (75), equation (74) can be written as:

$$\Delta_n = \frac{\beta(d_{SD} - d)}{\beta(d_{SD})} \left[\Delta'_n + 1\right] \left[\Delta'_n - 1\right] \tag{76}$$

where $\Delta'_n = \frac{1}{\sqrt{\beta(d)/\beta(d_{SD})}} + \frac{1}{\sqrt{\beta(d_{SD}-d)/\beta(d_{SD})}}$ while $\beta_{0,N_r+1} = \beta(d_{SD})$. Typical plots of the function $\frac{1}{\sqrt{\beta(d)/\beta(d_{SD})}}$ versus the normalized distance $\frac{d}{d_{SD}}$ are provided in Fig. 10. The analysis of this function shows that it is always above the first bisector. Note that while the results in Fig. 10 are provided for $C_n^2 = 1.7{\times}10^{-14}$ m$^{-2/3}$, similar variation trends were reported for all values of C_n^2. Consequently:

$$\frac{1}{\sqrt{\beta(d)/\beta(d_{SD})}} \geq \frac{d}{d_{SD}} \tag{77}$$

and $\frac{1}{\sqrt{\beta(d_{SD}-d)/\beta(d_{SD})}} \geq \frac{d_{SD}-d}{d_{SD}}$ implying that $\Delta'_n \geq 1$. Therefore, the third term in (76) is positive. Given that the first two terms are always positive, then $\Delta_n \geq 0$. Replacing this inequality in (73) implies that $\nu_{MIMO} - \nu_R > 0$ completing the proof of proposition 2.

REFERENCES

[1] M. Safari and M. Uysal, "Do we really need OSTBCs for free-space optical communication with direct detection?" *IEEE Trans. Wireless Commun.*, vol. 7, no. 11, pp. 4445 – 4448, November 2008.

[2] S. G. Wilson, M. Brandt-Pearce, Q. Cao, and J. H. Leveque, "Free-space optical MIMO transmission with Q-ary PPM," *IEEE Trans. Commun.*, vol. 53, pp. 1402–1412, August 2005.

[3] A. Garcia-Zambrana, C. Castillo-Vazquez, B. Castillo-Vazquez, and A. Hiniesta-Gomez, "Selection transmit diversity for FSO links over strong atmospheric turbulence channels," *IEEE Photon. Technol. Lett.*, vol. 21, pp. 1017 – 1019, July 2009.

[4] C. Abou-Rjeily, "On the optimality of the selection transmit diversity for MIMO-FSO links with feedback," *IEEE Commun. Lett.*, vol. 15, no. 6, pp. 641 – 643, June 2011.

[5] M. Karimi and M. Nasiri-Kenari, "BER analysis of cooperative systems in free-space optical networks," *J. Lightwave Technol.*, vol. 27, no. 24, pp. 5639–5647, December 2009.

[6] A. Garcia-Zambrana, C. Castillo-Vasquez, B. Castillo-Vasquez, and R. Boluda-Ruiz, "Bit detect and forward relaying for FSO links using equal gain combining over gamma-gamma atmospheric turbulence channels with pointing errors," *Opt. Express*, vol. 20, no. 15, pp. 16 394 – 16 409, July 2012.

[7] C. Abou-Rjeily and A. Slim, "Cooperative diversity for free-space optical communications: Transceiver design and performance analysis," *IEEE Trans. Commun.*, vol. 59, no. 3, pp. 658–663, March 2011.

[8] M. R. Bhatnagar, "Performance analysis of decode-and-forward relaying in gamma-gamma fading channels," *IEEE Photon. Technol. Lett.*, vol. 24, no. 7, pp. 545 – 547, April 2012.

[9] M. Feng, J. Wang, M. Sheng, L. Cao, X. Xie, and M. Chen, "Outage performance for parallel relay-assisted free-space optical communications in strong turbulence with pointing errors," in *International Conference on Wireless Commun. and Signal Proc.*, 2011, pp. 1 – 5.

[10] C. Abou-Rjeily, "Achievable diversity orders of decode-and-forward cooperative protocols over gamma-gamma fading FSO links," *IEEE Trans. Commun.*, vol. 61, no. 9, pp. 3919–3930, September 2013.

[11] S. Aghajanzadeh and M. Uysal, "Outage performance and DMT analysis of DF parallel relaying in FSO IM/DD communications," in *IEEE Vehicular Technology Conference*, 2012, pp. 1 – 5.

[12] M. Safari and M. Uysal, "Relay-assisted free-space optical communication," *IEEE Trans. Wireless Commun.*, vol. 7, no. 12, pp. 5441 – 5449, December 2008.

[13] M. Kashani and M. Uysal, "Outage performance of FSO multi-hop parallel relaying," in *IEEE Signal Processing and Commun. App. Conference*, 2012, pp. 1 – 4.

[14] M. Kashani, M. Safari, and M. Uysal, "Optimal relay placement in cooperative free-space optical communication systems," *IEEE J. Opt. Commun. Netw.*, vol. 5, no. 1, pp. 37 – 47, January 2013.

[15] N. D. Chatzidiamantis, D. S. Michalopoulos, E. E. Kriezis, G. K. Karagiannidis, and R. Schober, "Relay selection protocols for relay-assisted free-space optical systems," *IEEE J. Opt. Commun. Netw.*, vol. 5, no. 1, pp. 4790 –4807, January 2013.

[16] C. Abou-Rjeily and S. Haddad, "Cooperative FSO systems: Performance analysis and optimal power allocation," *J. Lightwave Technol.*, vol. 29, no. 7, pp. 1058–1065, April 2011.

[17] C. Abou-Rjeily, "Performance analysis of selective relaying in cooperative free-space optical systems," *J. Lightwave Technol.*, vol. 31, no. 18, pp. 2965–2973, September 2013.

[18] Y. Dhungana and C. Tellambura, "New simple approximations for error probability and outage in fading," *IEEE Commun. Lett.*, vol. 16, no. 11, pp. 1760–1763, November 2012.

[19] L. Zheng and D. N. C. Tse, "Diversity and multiplexing: A fundamental tradeoff in multiple-antenna channels," *IEEE Trans. Inform. Theory*, vol. 49, no. 5, pp. 1073–1096, May 2003.

[20] The wolfram functions site. [Online]. Available: http://functions.wolfram.com/Bessel-TypeFunctions/BesselK/06/ShowAll.html

[21] M.-A. Khalighi, N. Schwartz, N. Aitamer, and S. Bourennane, "Fading reduction by aperture averaging and spatial diversity in optical wireless systems," *IEEE Journal of Optical Commun. and Networking*, vol. 1, pp. 580 – 593, November 2009.

[22] P. Kaur, V. Jain, and S. Kar, "Capacity of free space optical links with spatial diversity and aperture averaging," in *Proceedings Biennial Symposium on Communications*, 2014, pp. 14 – 18.